AGU ADVANCING EARTH AND SPACE SCIENCE

Geophysical Research Letters

RESEARCH LETTER
10.1029/2020GL087624

# Summertime Temperature Variability Increases With Local Warming in Midlatitude Regions

**Duo Chan[1], Alison Cobb[2], Lucas R. Vargas Zeppetello[3], David S. Battisti[3], and Peter Huybers[1]**

[1]Department of Earth and Planetary Sciences, Harvard University, Cambridge, MA, USA, [2]Department of Physics, Imperial College London, London, UK, [3]Department of Atmospheric Sciences, University of Washington, Seattle, WA, USA

**Key Points:**
- Summertime temperature variability and warming in NH midlatitudes covary across CMIP5 models, especially in Europe
- Such covariance between warming and increased variability accentuates risks of future high-temperature events
- Albeit a weaker relationship than with warming, increases in variability also scale with biases in simulated historical variability

**Supporting Information:**
- Supporting Information S1

**Correspondence to:**
D. Chan,
duochan@g.harvard.edu

**Citation:**
Chan, D., Cobb, A., Zeppetello, L. R. V., Battisti, D. S., & Huybers, P. (2020). Summertime temperature variability increases with local warming in midlatitude regions. *Geophysical Research Letters*, *47*, e2020GL087624. https://doi.org/10.1029/2020GL087624

Received 25 FEB 2020
Accepted 26 MAY 2020
Accepted article online 9 JUN 2020

**Abstract** Climate change presents risks both in terms of warming and increased variability that are heightened when compounded. It is thus notable that the simulations in the Coupled Model Intercomparison Project Phase 5 (CMIP5) showing greater Northern midlatitude continental warming also show a greater increase in monthly average temperature variance, particularly in Europe. European variability increases with warming at a rate of 0.40°C$^2$/°C (95% C.I. [0.28, 0.50]), with local warming rates explaining 71% of the intermodel difference in variability changes. Coupling between warming and variance increases the probability of high temperatures compared to a scenario where variance is stable. If warming were to reach 6°C, the risk of monthly average temperature exceeding a 30°C threshold is 4 times greater in the increased-variance scenario. Despite the simple scaling across models suggesting some common origin, changes in model temperature and variance potentially involve a range of mechanisms whose contributions remain unclear.

**Plain Language Summary** Extreme and persistent summertime temperatures present risks to human health, property, and natural systems. The frequency of hot extremes increases in response to both growing mean temperature and increasing variability. Here we show that models that predict higher summertime warming also predict greater increases in temperature variability in midlatitude continents, especially in Europe. The combination of warming and increased variability makes the chances of hot extremes much greater than if temperature variance stayed constant. The reasons for increased variability may involve changes in soil moisture, variability in local radiation, and changes in atmospheric circulation, but exactly why a simple scaling between warming and increased variance emerges in Europe and elsewhere is unclear.

## 1. Introduction

In a warming climate, changes in the frequency of extreme events can result from a growing mean temperature, increased temperature variability, or a combination of both (Barriopedro et al., 2011; Beniston & Diaz, 2004; Della-Marta et al., 2007; Donat & Alexander, 2012; Hegerl et al., 2004; Schär et al., 2004). Historically, despite an unarguable increasing mean temperature, summertime temperature variance has not yet shown significant changes (Huntingford et al., 2013; Rhines & Huybers, 2013). It follows that the increased frequency of observed extreme temperature events is attributable to growing mean temperatures, as opposed to increased variability (Coumou et al., 2013; Griffiths et al., 2005; Simolo et al., 2011). Climate simulations, however, generally project increased summertime temperature variance in midlatitude continents (Fischer & Schär, 2009; Gregory & Mitchell, 1995; Holmes et al., 2016; Rowell, 2005; Scherrer et al., 2005).

Projections of variance differ across models (Fischer & Schär, 2009; Fischer et al., 2012; Holmes et al., 2016) for a variety of reasons (Christensen et al., 2008). The mechanism that has received the most attention involves changes in soil moisture (Koster et al., 2004, 2006) and the consequences for the partition of sensible and latent fluxes in the surface energy budget (Lenderink et al., 2007; Orth & Seneviratne, 2017; Seneviratne et al., 2006, 2010). Soil moisture, for example, has been indicated as important for accurate simulation of modern summertime variability (Fischer et al., 2012; Merrifield, 2016) and lack thereof is thought to have increased the strength and duration of both European and Russian heatwaves (Fischer et al., 2007; Rasmijn et al., 2018). Changes in radiative forcing associated with cloud cover (Lenderink et al., 2007;

Pfahl & Wernli, 2012) and thermal advection associated with changes in temperature gradients and circulation patterns (Holmes et al., 2016; van Ulden & van Oldenborgh, 2006) may also influence changes in variance.

## 2. Data and Methods

We examine the relationship between summertime warming and changes in variability in the midlatitudes using observations and simulations from the Coupled Model Intercomparison Project Phase 5 (CMIP5) (Taylor et al., 2012). Simulations of monthly summertime (June–August, JJA) near-surface air temperature are examined from 23 CMIP5 models (for a list of models used in this study, see legend in Figure 2a). We focus on monthly temperature variance because we are interested in coherent and persistent temperature anomalies that can potentially lead to strong social or biological impacts (Fischer et al., 2012; Holmes et al., 2016).

A single ensemble member (i.e., r1i1p1) is analyzed from each model, with output regridded to a common 2.5° resolution. Models whose original resolution is coarser than 2.5° are excluded because interpolating to finer resolution may bias variability estimates low (Hawkins & Sutton, 2012). We analyze two 30-year periods of model output—1976–2005 from the historical all-forcing experiment (hereafter historical) and 2071–2100 from the RCP8.5 experiment (hereafter RCP8.5). Linear trends are removed from each month for individual 30-year periods before calculating temperature variance.

A linear model is used to examine whether variability changes covary significantly with local changes in mean temperatures,

$$\Delta\sigma^2 = \alpha\Delta T + \beta, \tag{1}$$

where $\Delta\sigma^2$ and $\Delta T$ are changes in variance and temperature, respectively. The $\alpha$ is a scaling factor and $\beta$ is an intercept. The fact that $\Delta T$ is itself uncertain will generally lead to regression dilution when using a standard least squares approach. To help minimize regression dilution effects, we use a York regression technique (York et al., 2004).

York regression requires uncertainties of $\Delta T$ and $\Delta\sigma^2$, which are estimated using a 2-year (i.e., two consecutive intervals of JJA) block bootstrapping technique wherein detrended time series are resampled with replacements 100 times (Kunsch, 1989; McKinnon et al., 2017). Block bootstrapping retains the spatial covariance structure of the data (McKinnon et al., 2017) such that uncertainties of spatially averaged quantities are not biased low. Results are insensitive to the length of the blocks. The uncertainty of York fit slopes are estimated by bootstrapping individual models with replacement and repeating 100,000 times.

## 3. Results

In RCP8.5 experiments, all CMIP5 models predict warming over all land, with enhanced warming (> 5°C) seen in central North America and Europe (Figure 1a). Though models all agree on the sign of change, the magnitude of warming remains uncertain, especially poleward of 40°N (Figure 1c). The interquartile range of warming reaches 3–4°C in Central North America, Southern Europe, and Southwest Russia. Conversely, the warming rates in arid regions (e.g., the Sahara and Gobi desserts) are in good agreement with an interquartile range of less than 2°C (Figure 1c), despite cross-model average warming of 6°C, indicative of the importance of water in soils and clouds in determining regional sensitivity.

Changes in variability are more uncertain than changes in the mean across CMIP5 models. Averaged over midlatitude land masses, the interquartile range of changes in variance is 0.82°C$^2$ (Figure 1d), whereas the average increase in variance is only 0.27°C$^2$ (Figure 1b), such that the interquartile range of variability change encompasses zero in most regions. Even in Central Europe and Western Russia, where more than 75% models agree in terms of the sign of variability change and the multimodel average variability has the largest increase of ~1.5°C$^2$, the interquartile range is more than 2°C$^2$. The CMIP5 pattern of variability increase in Europe is similar to earlier regional model simulations, that is, the CHRM RCM (Schär et al., 2004) and PRUDENCE ensembles (Fischer et al., 2012), though differs from another ensemble that indicates greater increases in variance in Southern Europe, that is, ENSEMBLES (Fischer et al., 2012). When

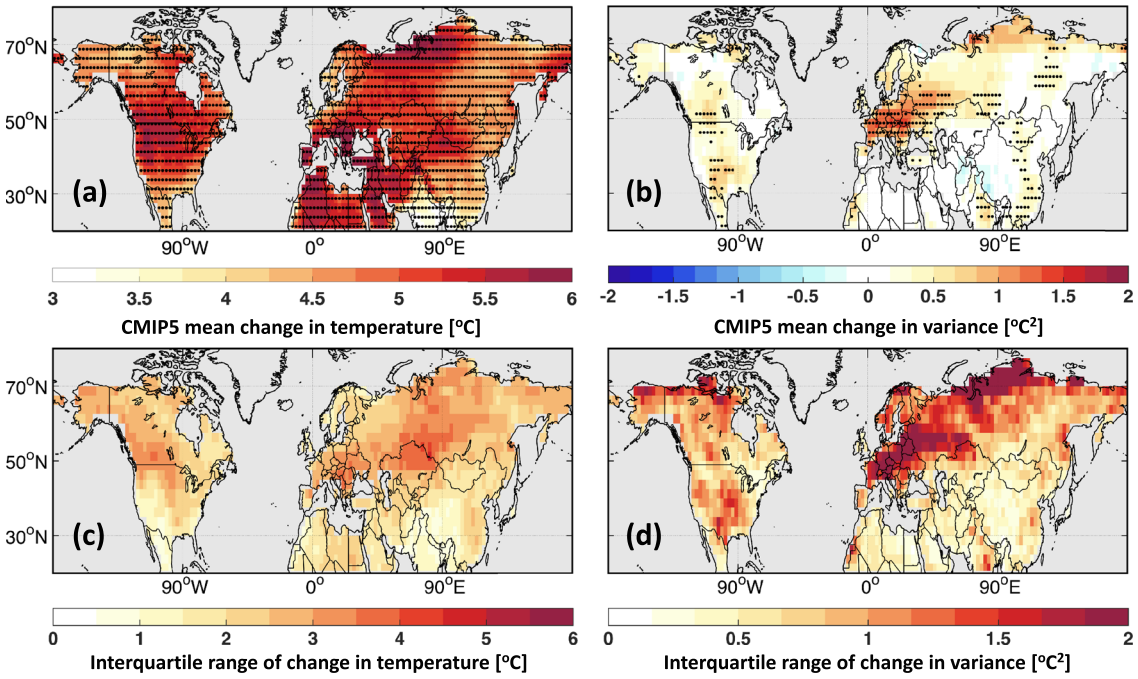


**Figure 1.** Projections of changes in summertime mean temperature and variability are uncertain across models. (a) Multimodel mean change in 30-year mean temperature (2071–2100 minus 1976–2005). Dots denote that more than 17 (75%) models have the same sign of change. (b) As in (a) but for multimodel mean change in temperature variance. (c) Interquartile range of changes in mean temperature across 23 models. (d) As in (c) but for changes in temperature variability.

converted to a percentage of change in standard deviation, CMIP5 models, on average, increase by 30–35%, whereas increases in earlier simulations exceed 60% (Fischer et al., 2012; Schär et al., 2004).

It is both interesting and concerning that a positive, linear scaling emerges between uncertain predictions of mean warming and variance in certain regions (Figure 2a). The largest scaling is seen in Europe where variance increases by 0.40°C$^2$/°C (95% C.I. [0.28, 0.50]; Figure 2b). The squared cross-model correlation between local warming and change in variability is 0.71, suggesting a strong linear dependence. When our analysis includes multiple ensemble members for some CMIP5 models, the scaling between European warming and variability change remains its central estimate of 0.40°C$^2$/°C, though the 95% C.I. slightly increases to [0.27, 0.51] (see Figure S1 in the supporting information). Scherrer et al. (2005) reported an insignificant positive relationship between increases in European standard deviation and warming across seven CMIP3 models, having an ordinary least squares slope of 0.05°C/°C (95% C.I. [− 0.04, 0.14]). The slope for CMIP5 models, if computed using standard deviations and ordinary least squares, is 0.10°C/°C (95% C.I. [0.07, 0.13]). A major difference in our findings is the appearance of significant scaling between European warming and change in either standard deviation or variance, which apparently stems from a stronger relationship across CMIP5 models and is robust to the choice of ordinary least squares or York methods. In addition to the strong relationship in Europe, weaker but still significant positive relationships are also found in Southern Canada, the Southeastern United States, and Southeast China.

Insomuch as the emergent scaling between variance and warming holds, Europe and other continental regions in the Northern Hemisphere face a compound risk whereby exposure to high temperatures is heightened both on account of mean warming and increased variance. To estimate how compounding warming and variance increase the risk of extreme hot months in Europe, we compare two scenarios. In a fixed case, we vary the warming rate in the range of CMIP5 projections from 2°C to 8°C, but keep the variance at the historical multi-model average of 2.53°C$^2$. In a second case, we prescribe a variance that linearly increases with warming, $\Delta\sigma^2 = 0.40\Delta T - 1.33$, where the relationship is the best estimate from the York fit (red line in Figure 2b). Moreover, we assume that monthly temperatures follow Gaussian distributions and use the Gaussian cumulative density function to calculate the probability of monthly temperatures exceeding some thresholds (Figure 3a).

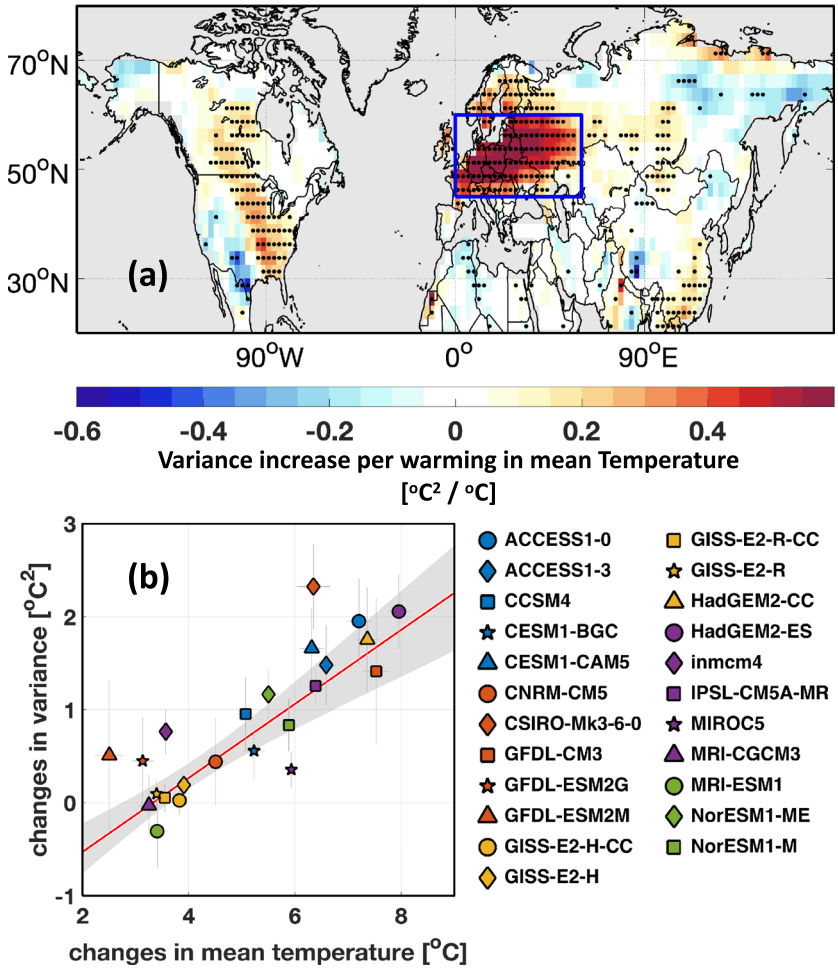


**Figure 2.** Variability change and local warming. (a) Changes in temperature variance per warming of mean temperature estimated by a York regression technique. Dots indicate significance at the 95% level by bootstrapping individual models. (b) Changes in variance versus warming of mean temperature in Europe (blue box in panel a). One standard deviation uncertainties are estimated for individual models (error bars on each marker) using 2-year block bootstrapping. The central estimate of a York regression (red line) explains 71% ($r^2$) of intermodel variance in variability change and the associated 95% coverage interval (gray shading) is estimated by bootstrapping individual models.

How warming and increased variance combine to increase the frequency of extreme hot months can be illustrated with respect to a 6°C warming and a 30°C exceedance threshold (Figure 3a). The regression across CMIP5 models (Figure 2) indicates that a 6°C warming, which is near the average across the 23 models, will cause an 1.1°C$^2$ increase in variance from 2.5°C$^2$ to 3.6°C$^2$ (95% C.I., [3.3, 3.9]). With this warming and increased variance, the probability of a monthly temperature exceeding a 30°C threshold is 0.8%. If variance were instead held fixed, the probability is only 0.2%. Translating into a return period, or the inverse of the exceedance probability, gives 132 summer months when variance compounds with warming versus 539 when variance is fixed.

More generally, we consider how return period changes with local warming and temperature threshold (Figure 3b). In a case where variance is fixed, contour lines of return period follow a one-to-one relationship between mean warming and threshold. In the compounding case, however, slopes of contour lines are approximately 1.3 times as steep relative to when variance is fixed. For warming greater than 6.2°C and a temperature threshold above 31.5°C, the return periods for the compounding case are more than an order of magnitude smaller than for the fixed case. Note that return periods are calculated under the presumption of Gaussian variability, but there is evidence that the distribution of summer temperature variability alters with warming (Huybers et al., 2014; Volodin & Yurova, 2013).

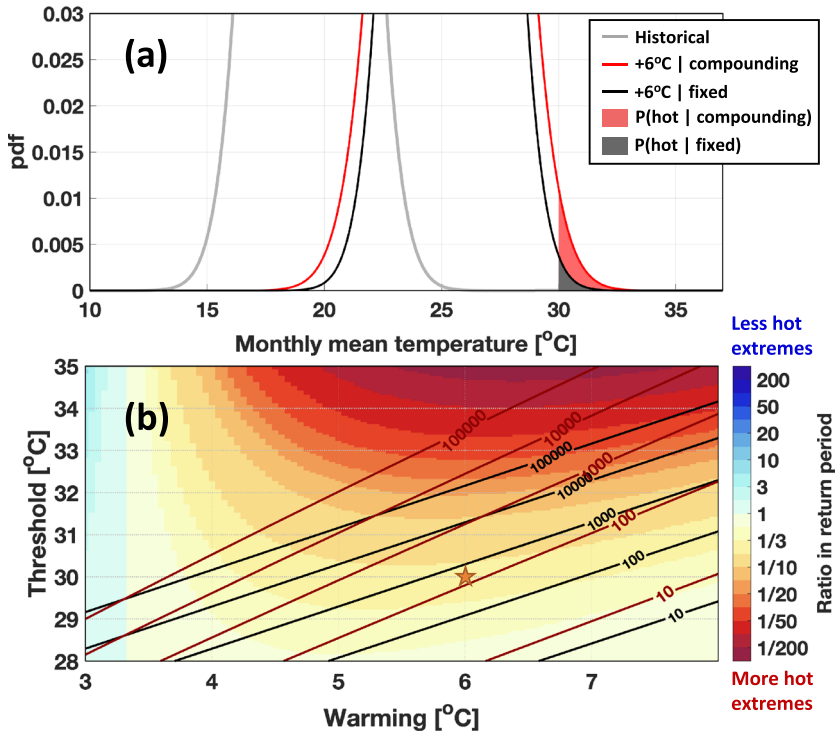


**Figure 3.** Compounding risk increases the probability of extreme hot months. (a) Probability density function of monthly temperature for historical (black solid) and 6° C warming scenarios (gray) in Europe. Monthly temperatures are assumed to follow Gaussian distributions. The case where variability compounds with warming (red) is compared with a case where variability is fixed (black). When warming is 6°C (red star in panel b), the probability of monthly temperature exceeding 30°C in the compounding case (red shading) is four times of that in a fixed cased (gray shading). (b) Ratio in return periods (shading) between the compounding and the fixed case under a variety of warming rates and thresholds for extreme hot months. A smaller ratio indicates that extreme hot months are more likely to happen in the compounding case. Note that the color bar is nonlinear. Return periods are shown as contour lines (up to 100 K summer months) for the compounding (red) and the fixed case (black).

It is useful to inquire whether other quantities, in addition to local warming, permit for predicting changes in variability across models. Using a collection of regional climate simulations, Fischer et al. (2012) showed that increasing model biases in simulated summer temperature variability leads to a decrease in predicted changes. They suggested that models having larger historical variance are drier in the modern climate and, therefore, have limited potential for further drying and consequent increases in temperature variability. In contrast, using CMIP5, we find variability change to increase with historical biases by 0.89 $°C^2/°C^2$ in Europe (95% C.I. [0.54, 1.30], Figure S2e). Historical biases, however, only explain 12% of intermodel spread in variability change. Similar positive but weak relationships between variability change and historical biases are found in Western Russia, Southern Canada, Eastern United States, and Southeast China (Figure S2d). Here, historical biases are calculated relative to observational variance from CRUTS Version 4 (Harris et al., 2014), and results are consistent if the University of Delaware data set (Willmott & Matsuura, 2001) or ERA-Interim reanalysis (Dee et al., 2011) are used as observations.

## 4. Discussion and Conclusions

Although a quantitative and deterministic analysis for mechanisms that relates local warming and variability change is beyond the scope of this current paper, we discuss below the role of several possible processes, including soil moisture, radiative forcing, and thermal advection. A variety of mechanisms involve soil moisture. Large scale drying is a common feature in CMIP5 model simulations (Berg et al., 2017), and changes in soil dryness correlate with mean warming in Europe across CMIP5 models (Berg & Sheffield, 2018). Moreover, interannual temperature variability also increases with dryness across CMIP5 models in historical simulations (Berg & Sheffield, 2018). Thus, if soil moisture is the dominating mechanism, we expect that the models that dry more will have both increased temperature and variability. Interestingly,

the *y* intercept between warming and changes in variability is not at 0 but − 1.33 (95% C.I. [− 1.76, − 0.80]). Models that produce only approximately 3°C of warming in response to increased greenhouse gas forcing have essentially no change in temperature variance. In other words, only models showing strong warming has a distinct change in variance, which is consistent with the mechanism of soil moisture.

Another candidate is the variability of radiative imbalance, which can lead to temperature differences without changes in moisture. Radiative imbalances are often associated with changes in cloud and precipitation (Vargas Zeppetello et al., 2019), which are often considered as a part of large-scale circulation patterns (Andrade et al., 2012) but are also closely related to local changes in soil moisture (Berg & Sheffield, 2018). In considering the causes of changes in variance, we should not consider changes in soil moisture and atmospheric circulation as being independent. For example, Rasmijn et al. (2018) show that the frequency of extreme hot temperatures increases because of circulation patterns that tend to induce drying soil. As a result, a better understanding of changes in large-scale rainfall patterns among distinct GCMs, together with the causes of changes in radiative and rainfall variability, seems important.

The third possibility is thermal advection associated with changes in either temperature gradients or wind variability. Holmes et al. (2016) found limited (less than 25%) contributions from thermal advection to summertime temperature variance using an ensemble of simulations from a single model. In CMIP5 simulations, we find that the magnitude of the temperature gradient increases on the order of 0.05°C per 100 km across midlatitudes between 1976–2005 and 2071–2100, whereas the climatological temperature gradient is on the order of 0.5°C per 100 km. Consistent with Holmes et al. (2016), such a change in gradient appears too weak to explain changes in variance of $1.5°C^2$ (~40% variance increase compared with the 1976–2005 baseline period). We also analyze 30 years of ERA-Interim Reanalysis data (Dee et al., 2011) and found that the influence of thermal advection on local summertime temperature variability is weak outside of coastal regions. We, therefore, expect changes in thermal advection to play a limited role in modifying variability.

In conclusion, a strong linear relationship between warming and predicted increases in variability exists in Europe and other mid-latitude regions across CMIP5 models. This result indicates compounded risks of exposure to extreme hot months: If climate sensitivity is high so will be variance. Such risks highlight the importance of further constraining climate sensitivity at regional and seasonal scales, and better determining the causal mechanisms associated with increased summertime temperature variability.

## Data Availability Statement

Data sets for this research are available in this in-text data citation reference: Taylor et al. (2012), with license of CMIP5. Codes and processed data for generating figures and statistics in this study are posted online (https://doi.org/10.5281/zenodo.3832927).

**Acknowledgments**
This research began at the Advanced Climate Dynamics Course in 2017. D. C. and P. H. were supported by the Harvard Global Institute. D. S. B. was supported by a grant from the Tamaki Foundation, and L. R. V. Z. was supported by a NSF GRFP fellowship.

## References

Andrade, C., Leite, S. M., & Santos, J. A. (2012). Temperature extremes in Europe: Overview of their driving atmospheric patterns. *Natural Hazards and Earth System Sciences*, *12*(5), 1671.

Barriopedro, D., Fischer, E. M., Luterbacher, J., Trigo, R. M., & García-Herrera, R. (2011). The hot summer of 2010: Redrawing the temperature record map of Europe. *Science*, *332*(6026), 220–224.

Beniston, M., & Diaz, H. F. (2004). The 2003 heat wave as an example of summers in a greenhouse climate? Observations and climate model simulations for Basel, Switzerland. *Global and Planetary Change*, *44*(1-4), 73–81.

Berg, A., & Sheffield, J. (2018). Soil moisture–evapotranspiration coupling in CMIP5 models: Relationship with simulated climate and projections. *Journal of Climate*, *31*(12), 4865–4878.

Berg, A., Sheffield, J., & Milly, P. C. D. (2017). Divergent surface and total soil moisture projections under global warming. *Geophysical Research Letters*, *44*, 236–224. https://doi.org/10.1002/2016GL071921

Christensen, J. H., Boberg, F., Christensen, O. B., & Lucas-Picher, P. (2008). On the need for bias correction of regional climate change projections of temperature and precipitation. *Geophysical Research Letters*, *35*, L20709. https://doi.org/10.1029/2008GL035694

Coumou, D., Robinson, A., & Rahmstorf, S. (2013). Global increase in record-breaking monthly-mean temperatures. *Climatic Change*, *118*(3-4), 771–782.

Dee, D. P., Uppala, S. M., Simmons, A. J., Berrisford, P., Poli, P., Kobayashi, S., et al. (2011). The ERA-Interim reanalysis: Configuration and performance of the data assimilation system. *Quarterly Journal of the Royal Meteorological Society*, *137*(656), 553–597.

Della-Marta, P. M., Haylock, M. R., Luterbacher, J., & Wanner, H. (2007). Doubled length of western European summer heat waves since 1880. *Journal of Geophysical Research*, *112*, D15103. https://doi.org/10.1029/2007JD008510

Donat, M. G., & Alexander, L. V. (2012). The shifting probability distribution of global daytime and night-time temperatures. *Geophysical Research Letters*, *39*, L14707. https://doi.org/10.1029/2012GL052459

Fischer, E. M., Rajczak, J., & Schär, C. (2012). Changes in European summer temperature variability revisited. *Geophysical Research Letters*, *39*, L19702. https://doi.org/10.1029/2012GL052730

Fischer, E. M., & Schär, C. (2009). Future changes in daily summer temperature variability: Driving processes and role for temperature extremes. *Climate Dynamics*, *33*(7-8), 917.
Fischer, E. M., Seneviratne, S. I., Vidale, P. L., Luthi, D., & Schär, C. (2007). Soil moisture–atmosphere interactions during the 2003 European summer heat wave. *Journal of Climate*, *20*(20), 5081–5099.
Gregory, J. M., & Mitchell, J. F. B. (1995). Simulation of daily variability of surface temperature and precipitation over europe in the current and 2×$CO_2$ climates using the UKMO climate model. *Quarterly Journal of the Royal Meteorological Society*, *121*(526), 1451–1476.
Griffiths, G. M., Chambers, L. E., Haylock, M. R., Manton, M. J., Nicholls, N., Baek, H.-J., et al. (2005). Change in mean temperature as a predictor of extreme temperature change in the Asia–Pacific region. *International Journal of Climatology: A Journal of the Royal Meteorological Society*, *25*(10), 1301–1330.
Harris, I. P. D. J., Jones, P. D., Osborn, T. J., & Lister, D. H. (2014). Updated high-resolution grids of monthly climatic observations—The CRU TS3 10 dataset. *International Journal of Climatology*, *34*(3), 623–642.
Hawkins, E., & Sutton, R. (2012). Time of emergence of climate signals. *Geophysical Research Letters*, *39*, L01702. https://doi.org/10.1029/2011GL050087
Hegerl, G. C., Zwiers, F. W., Stott, P. A., & Kharin, V. V. (2004). Detectability of anthropogenic changes in annual temperature and precipitation extremes. *Journal of Climate*, *17*(19), 3683–3700.
Holmes, C. R., Woollings, T., Hawkins, E., & De Vries, H. (2016). Robust future changes in temperature variability under greenhouse gas forcing and the relationship with thermal advection. *Journal of Climate*, *29*(6), 2221–2236.
Huntingford, C., Jones, P. D., Livina, V. N., Lenton, T. M., & Cox, P. M. (2013). No increase in global temperature variability despite changing regional patterns. *Nature*, *500*(7462), 327.
Huybers, P., McKinnon, K. A., Rhines, A., & Tingley, M. (2014). US daily temperatures: The meaning of extremes in the context of non-normality. *Journal of Climate*, *27*(19), 7368–7384.
Koster, R. D., Dirmeyer, P. A., Guo, Z., Bonan, G., Chan, E., Cox, P., et al. (2004). Regions of strong coupling between soil moisture and precipitation. *Science*, *305*(5687), 1138–1140.
Koster, R. D., Suarez, M. J., & Schubert, S. D. (2006). Distinct hydrological signatures in observed historical temperature fields. *Journal of Hydrometeorology*, *7*(5), 1061–1075.
Kunsch, H. R. (1989). The jackknife and the bootstrap for general stationary observations. *The annals of Statistics*, *17*, 1217–1241.
Lenderink, G., Van Ulden, A., Van den Hurk, B., & Van Meijgaard, E. (2007). Summertime inter-annual temperature variability in an ensemble of regional model simulations: Analysis of the surface energy budget. *Climatic Change*, *81*(1), 233–247.
McKinnon, K. A., Poppick, A., Dunn-Sigouin, E., & Deser, C. (2017). An "observational large ensemble" to compare observed and modeled temperature trend uncertainty due to internal variability. *Journal of Climate*, *30*(19), 7585–7598.
Merrifield, X. S.-P. (2016). Summer u.s. air temperature variability: Controlling factors and AMIP simulation biases. *Journal of Climate*, *29*(14), 5123–5139.
Orth, R., & Seneviratne, S. I. (2017). Variability of soil moisture and sea surface temperatures similarly important for warm-season land climate in the community earth system model. *Journal of Climate*, *30*(6), 2141–2162.
Pfahl, S., & Wernli, H. (2012). Quantifying the relevance of atmospheric blocking for co-located temperature extremes in the Northern Hemisphere on (sub-) daily time scales. *Geophysical Research Letters*, *39*, L12807. https://doi.org/10.1029/2012GL052261
Rasmijn, L. M., Van der Schrier, G., Bintanja, R., Barkmeijer, J., Sterl, A., & Hazeleger, W. (2018). Future equivalent of 2010 Russian heatwave intensified by weakening soil moisture constraints. *Nature Climate Change*, *8*(5), 381–385.
Rhines, A., & Huybers, P. (2013). Frequent summer temperature extremes reflect changes in the mean, not the variance. *Proceedings of the National Academy of Sciences*, *110*(7), E546–E546.
Rowell, D. P. (2005). A scenario of european climate change for the late twenty-first century: Seasonal means and interannual variability. *Climate Dynamics*, *25*(7-8), 837–849.
Schär, C., Vidale, P. L., Lüthi, D., Frei, C., Häberli, C., Liniger, M. A., & Appenzeller, C. (2004). The role of increasing temperature variability in European summer heatwaves. *Nature*, *427*(6972), 332.
Scherrer, S. C., Appenzeller, C., Liniger, M. A., & Schär, C. (2005). European temperature distribution changes in observations and climate change scenarios. *Geophysical Research Letters*, *32*, L19705. https://doi.org/10.1029/2005GL024108
Seneviratne, S. I., Corti, T., Davin, E. L., Hirschi, M., Jaeger, E. B., Lehner, I., et al. (2010). Investigating soil moisture–climate interactions in a changing climate: A review. *Earth-Science Reviews*, *99*(3-4), 125–161.
Seneviratne, S. I., Lüthi, D., Litschi, M., & Schär, C. (2006). Land–atmosphere coupling and climate change in Europe. *Nature*, *443*(7108), 205.
Simolo, C., Brunetti, M., Maugeri, M., & Nanni, T. (2011). Evolution of extreme temperatures in a warming climate. *Geophysical Research Letters*, *38*, L16701. https://doi.org/10.1029/2011GL048437
Taylor, K. E., Stouffer, R. J., & Meehl, G. A. (2012). An overview of CMIP5 and the experiment design. *Bulletin of the American Meteorological Society*, *93*(4), 485–498.
van Ulden, A. P., & van Oldenborgh, G. J. (2006). Large-scale atmospheric circulation biases and changes in global climate model simulations and their importance for climate change in Central Europe. *Atmospheric Chemistry and Physics*, *6*, 863–881.
Vargas Zeppetello, L. R., Battisti, D. S., & Baker, M. B. (2019). The origin of soil moisture evaporation regimes. *Journal of Climate*, *32*(20), 6939–6960.
Volodin, E. M., & Yurova, A. Y. (2013). Summer temperature standard deviation, skewness and strong positive temperature anomalies in the present day climate and under global warming conditions. *Climate dynamics*, *40*(5-6), 1387–1398.
Willmott, C. J., & Matsuura, K. (2001). Terrestrial air temperature and precipitation: Monthly and annual climatologies (version 3.02). Center for Climatic Research, Department of Geography, University of Delaware.
York, D., Evensen, N. M., Martınez, M. L., & De Basabe Delgado, J. (2004). Unified equations for the slope, intercept, and standard errors of the best straight line. *American Journal of Physics*, *72*(3), 367–375.